Electronic structure of a Mn_{12} molecular magnet: Theory and experiment

D. W. Boukhvalov,[1] M. Al-Saqer,[2] E. Z. Kurmaev,[1] A. Moewes,[3] V. R. Galakhov,[1] L. D. Finkelstein,[1] S. Chiuzbăian,[4] M. Neumann,[5] V. V. Dobrovitski,[2] M. I. Katsnelson,[6,7] A. I. Lichtenstein,[7,8] B. N. Harmon,[2] K. Endo,[9] J. M. North,[10] and N. S. Dalal[10]

[1]*Institute of Metal Physics, Russian Academy of Sciences Ural Division, Ekaterinburg 620219, Russia*
[2]*Ames Laboratory, Iowa State University, Ames, Iowa 50011, USA*
[3]*Department of Physics and Engineering Physics, University of Saskatchewan, 116 Science Place, Saskatoon, Saskatchewan, Canada S7N 5E2*
[4]*Paul Scherrer Institut, CH-5232 Villigen PSI, Switzerland*
[5]*Fachbereich Physik, Universität Osnabrück, D-49069 Osnabrück, Germany*
[6]*Department of Physics, Uppsala University, Box 530, SE-751 21 Uppsala, Sweden*
[7]*University of Nijmegen, NL-6525 ED Nijmegen, The Netherlands*
[8]*Institute of Theoretical Physics, University of Hamburg, 20355 Hamburg, Germany*
[9]*Department of Chemistry, Faculty of Science, Kanazawa University, Kanazawa, Ishikawa 920-1192, Japan*
[10]*Department of Chemistry, Florida State University, Tallahassee, Florida 32306, USA*

(Received 7 June 2006; revised manuscript received 6 October 2006; published 12 January 2007)

We used site-selective and element-specific resonant inelastic x-ray scattering (RIXS) to study the electronic structure and the electron interaction effects in the molecular magnet $[Mn_{12}O_{12}(CH_3COO)_{16}(H_2O)_4]\cdot 2CH_3COOH\cdot 4H_2O$, and compared the experimental data with the results of local spin density approximation $+U$ electron structure calculations which include the on-site Coulomb interactions. We found a good agreement between theory and experiment for the Coulomb repulsion parameter $U=4$ eV. In particular, the p-d band separation of 1.8 eV has been found from the RIXS spectra, which is in accordance with the calculations. Similarly, the positions of the peaks in the XPS spectra agree with the calculated densities of p and d states. Using the results of the electronic structure calculations, we determined the intramolecular exchange parameters, and used them for diagonalization of the Mn_{12} spin Hamiltonian. The calculated exchanges gave the correct ground state with the total spin $S=10$.

DOI: 10.1103/PhysRevB.75.014419 PACS number(s): 75.50.Xx, 75.30.Et, 75.25.+z, 71.20.−b

I. INTRODUCTION

$[Mn_{12}O_{12}(CH_3COO)_{16}(H_2O)_4]\cdot 2CH_3COOH\cdot 4H_2O$ (in short, Mn_{12} acetate or Mn_{12}) synthesized by Lis[1] is one of the most well-investigated molecular magnets, and one where magnetization tunneling has been reported.[2,3] Every molecule of this compound contains eight Mn^{3+} ions with spin $S=2$, and four Mn^{4+} ions with spin $S=3/2$, which are held together by the oxygen atoms, acetate ligands, and the water of crystallization. The molecules of Mn_{12} form molecular crystals with a tetragonal lattice. The Mn ions inside a molecule are coupled by strong superexchange interactions which result in a ground state with a high total spin $S=10$ per molecule. Every molecule is surrounded by a crown of ligands, which makes the intermolecular magnetic couplings (mostly dipolar in origin) very weak. Thus, each molecule behaves as an almost isolated nanoscale magnetic particle. The molecular magnets, and Mn_{12} in particular, are very suitable objects for studying numerous aspects of nanoscale magnetism, such as quantum spin tunneling, spin relaxation of nanoscopic magnets, the implications of the topological spin phase (Berry phase), etc.[4–7] In comparison with other magnetic "zero-dimensional" nanosystems, such as nanoparticles, the molecular magnets have a number of advantages: they are highly monodisperse, they have regular single-crystal structure, and their properties often can be varied by very efficient and well-developed techniques of molecular chemistry.

In order to understand the magnetic properties at the intramolecular scale, it is important to investigate in detail the electronic structure of molecular nanomagnets, especially the electron correlation effects. In many transition metal-oxide systems, the standard density functional methods [local density approximation (LDA) or generalized gradient approximation] do not reproduce the energy gap and magnetic superexchange interactions,[8–10] and many-body effects should be taken into account at least in the simple form of the LDA+U approximation.[11] A somewhat similar situation takes place in magnetic molecules, where the transition metal ions are coupled by the oxygen bridges. The density functional computations of the electronic structure for Mn_{12} acetate[12–15] reproduce well the value of the magnetic moment and the easy axis anisotropy, but strongly underestimate the gap in the electron spectrum. Also, the intramolecular exchange interactions calculated for V_{15} magnetic molecules using the density functional theory (DFT) are strongly overestimated (by a factor of 3).[16] In contrast with the DFT calculations, the account of the on-site Coulomb interactions within the local spin density approximation (LSDA)+U approach gives the value of the gap, the main features of the band structure,[17,18] and (for the case of V_{15}) exchange parameters very close to the experiment.[17,19,20]

Therefore, an account of the Coulomb interactions is important for correct evaluation of the parameters of the intramolecular interactions. Unfortunately, the choice of the value for the parameter U, which determines the strength of

the on-site repulsion in the LDA+U (or LSDA+U) approach, is sometimes a very complicated problem.[11,21] Most of the existing methods are extremely difficult to apply for analysis of such a large and complex system as Mn_{12}, having about 150 atoms per unit cell. In the present paper it will be shown that consistent selection of the U parameter can be provided by comparison of LSDA+U calculations with resonant inelastic x-ray scattering (RIXS) spectra.

In our previous brief communication,[22] we reported RIXS spectra of Mn_{12} measured at the Mn L edge, and put forward a conjecture that U=4 eV has to be taken in order to achieve an agreement with the x-ray experiments. In the present paper, the previous measurements are completed, and the RIXS spectra measured at carbon and oxygen K edges allow us to distinguish the contribution of nonmetal $2p$ valence states from nonequivalent sites. In addition x-ray photoemission spectra (XPS) Mn $3s$ spectra of Mn_{12} are measured and are compared with spectra of reference samples; they are used for discussion of charge transfer from O $2p$ to Mn $3d$ states. Moreover, our initial conjecture is supported by extensive theoretical analysis, which includes (1) the calculation of the electronic structure of the full molecule, omitting only the intermolecular water of crystalization and solvate complexes; (2) theoretical estimate of the parameter U using constrained LDA calculations; (3) diagonalization of the resulting spin Hamiltonian and discussion of the spin excitation spectrum of Mn_{12}.

II. SAMPLE PREPARATION AND EXPERIMENTAL DETAILS

Polycrystalline samples of Mn_{12} were prepared as described in Refs. 1 and 23. Manganese acetate (99.99%), potassium permanganate (99%), and acetic acid (99.99%), as received from Aldrich, were used. Chemical analysis and magnetic measurements confirmed the purity of the prepared Mn_{12} samples.

The XPS measurements were carried out with a PHI 5600 ci multitechnique spectrometer using monochromatized Al $K\alpha$ radiation (E_{exc}=1486.6 eV). The estimated energy resolution is 0.35 eV, and the base pressure in the vacuum chamber during the measurements was about 5×10^{-9} Torr. The manganese $L_{2,3}$ ($3d4s\rightarrow2p_{1/2,3/2}$ transitions) and carbon and oxygen $K\alpha$ ($2p\rightarrow1s$ transition) x-ray emission spectra (XES) were recorded at the soft x-ray fluorescence end station on undulator beamline 8.0 at the Advanced Light Source at Lawrence Berkeley National Laboratory. The manganese $L_{2,3}$ and carbon and oxygen $K\alpha$ XES were measured resonantly through the manganese $L_{2,3}$ and carbon and oxygen K edges, and nonresonantly (far from thresholds). The energy resolution of the Mn L, C K, and O K spectra is about 0.8, 0.3, and 0.4 eV, respectively. The spectra are normalized to the number of incoming photons represented by a mesh current. The Mn $2p$, C $1s$, and O $1s$ x-ray absorption spectra were measured in the total electron yield mode.

III. DISCUSSION OF EXPERIMENTAL RESULTS

In RIXS, an incoming photon at first excites electrons from a core level to the conduction band.[24] This provides element specificity of the technique because of different binding energies associated with the core levels of different elements. Then an electron from the valence band recombines with the core hole, leaving an electron in the conduction band and a hole in the valence band. Since optical transitions obey the dipole selection rules, the RIXS spectra are also sensitive to the angular momentum of the states involved. Thus, measurements of XES and x-ray absorption spectra (XAS) at the Mn L edge give information about the local partial density of states (DOS) of the Mn $3d$ states, and measurements at the carbon and oxygen K edges provide similar information on the $2p$ states for both occupied and unoccupied levels. Local partial DOSs for each nonequivalent site occupied by the same chemical species (for instance, by nonequivalent carbon and oxygen atoms in Mn_{12}) can be distinguished by the measurements of RIXS using both energy[25] and angular[26] selection.

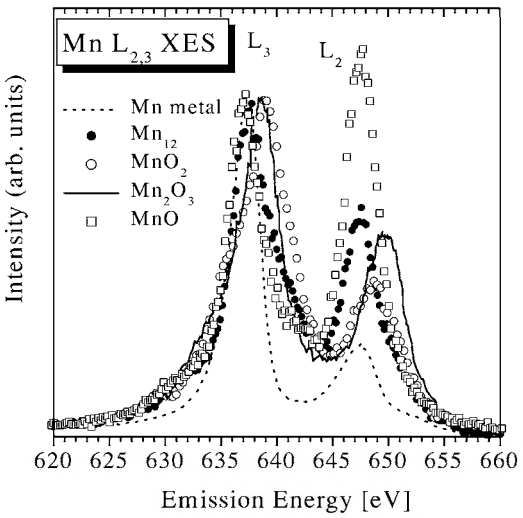

FIG. 1. The comparison of Mn $L_{2,3}$ XES of Mn_{12} with spectra of reference samples.

Soft x-ray emission and absorption spectra of Mn_{12} acetate are presented in Figs. 1–4. In Fig. 1, the nonresonant Mn $L_{2,3}$ XES of Mn_{12} (which correspond to Mn $3d4s\rightarrow2p_{1/2,3/2}$ transitions, and probe the occupied $3d4s$ states) are compared with the spectra of the Mn metal and the reference compounds (MnO, Mn_2O_3, and MnO_2). The ratio of the intensities $I(L_2)/I(L_3)$ is rather small for pure manganese metal, and deviates from the value of 0.5 expected from the j=3/2 and j=1/2 occupancy ratio due to the Coster-Kronig (CK) process $L_2L_3M_{4,5}$.[27] It is known that the $I(L_2)/I(L_3)$ intensity ratio increases on going from pure $3d$ metals to their oxides. This happens because the nonradiative $L_2L_3M_{4,5}$ CK transition probability is lower in $3d$ oxides than in metals.[28] As a result, the $I(L_2)/I(L_3)$ intensity ratio is highest for MnO ($\sim$1.1) with the band gap of 3.6–3.8 eV, and is lowest for Mn metal ($\sim$0.27).

According to Refs. 29 and 30, both the atomic magnetic moment and the Coster-Kronig effect are responsible for the $I(L_2)/I(L_3)$ intensity ratio in manganese compounds. The atomic magnetic moments of Mn^{3+} and Mn^{4+} ions in Mn_{12} are found to be close to those for Mn_2O_3 and MnO_2 (Ref. 31), respectively. Therefore, the increase of the ratio

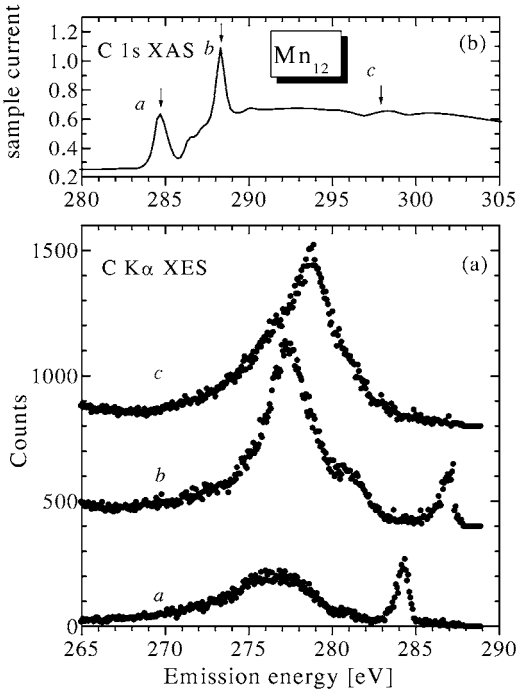

FIG. 2. RIXS spectra of Mn_{12} excited at C K edge.

$I(L_2)/I(L_3)$ for manganese compounds (as compared with metallic manganese) can be attributed to the weakening of the Coster-Kronig process due to higher localization of Mn $3d$ density in Mn_{12} in comparison with Mn_2O_3.

RIXS spectra of Mn_{12} excited at the carbon and oxygen K edges are presented in Figs. 2 and 3. In Fig. 2(a), we present the carbon $K\alpha$ ($2p \rightarrow 1s$ transition) XES measured at selected

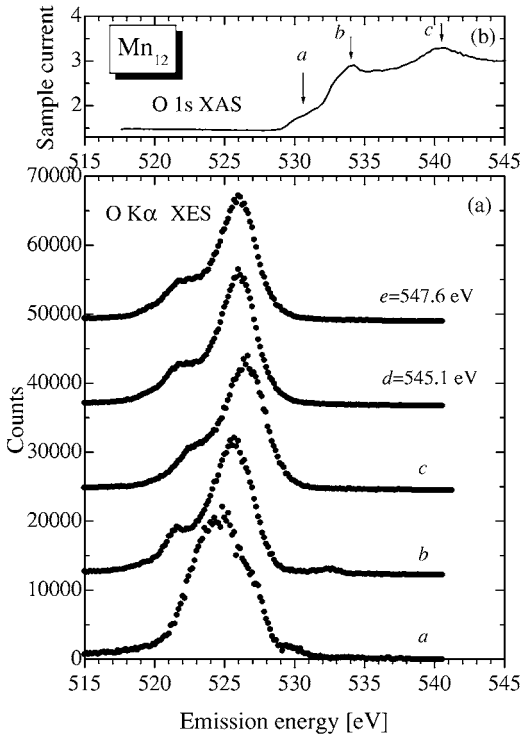

FIG. 3. RIXS spectra of Mn_{12} excited at O K edge.

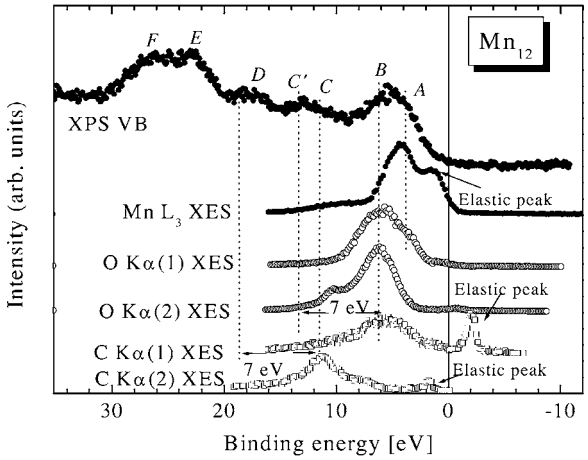

FIG. 4. The comparison of XPS VB and XES of constituents of Mn_{12} on the binding energy scale.

energies a and b; these energies correspond to the main peaks of carbon C $1s$ XAS [see Fig. 2(b)]. The C $K\alpha$ x-ray emission spectra [Fig. 2(a)] can be attributed to the contribution of nonequivalent carbon atoms in carboxylate groups (CH_3COO). This conclusion stems from our XPS measurements which demonstrate that the C $1s$ XPS of Mn_{12} is split into two lines with binding energies 283.7 and 288.6 eV, respectively.

The RIXS spectra of Mn_{12} excited at the O K edge (Fig. 3) show that the shape of the O $K\alpha$ XES strongly depends on the selected photon energies; the chosen energies correspond to the absorption peaks labeled a, b, and c. According to the XPS measurement, the O $1s$ spectrum of Mn_{12} consists of two peaks centered at 530.5 and 531.8 eV. These peaks can be attributed to the oxygen atoms linking the Mn atoms (the peak at 530.5 eV), and to the oxygen atoms belonging to the ligand water molecules and carboxylate groups (the peak at 531.8 eV). Based on this assignment, and taking into account the RIXS spectra of water,[32] we can attribute the origin of the absorption peaks a and b of the O $1s$ XAS of Mn_{12} [Fig. 3(a)] to the excitation of an oxygen $1s$ electron to the unoccupied $2p$ states belonging to the O1 and O2 atoms, respectively. The corresponding O $K\alpha$ XES selectively probes O $2p$ occupied states from the same nonequivalent oxygen atoms. The selectively excited O $K\alpha(1)$ and O $K\alpha(2)$ XES are attributed to different oxygen atoms. The first spectrum arises from the oxygens which link the Mn atoms in the $Mn_{12}O_{12}$, while the second one comes from the oxygens belonging to the ligand water molecules and to the carboxylates.

In Fig. 4, we compare the XES of the constituents with the XPS valence band (VB) on the binding energy scale taking into account the binding energies of the core levels. Based on this comparison, all features of XPS VB can be interpreted in the following way. Feature A originates from the contribution of the Mn $3d$ states, and feature B originates from the O $2p$ and C $2p$ states. Their energy difference is about 1.8 eV which means that they are strongly mixed, in accordance with the LSDA+U electronic structure calculations.[17] We note that our XPS VB is different from the spectrum given in Ref. 31 both in p-d mixing and in energy

calibration. Our XPS VB shows that the Mn 3*d* and O 2*p* states are strongly hybridized in Mn_{12}, and their overlap gives a rather broad XPS *p*-*d* peak located at ~5 eV. The energy separation of 1.8 eV between the Mn 3*d* and O 2*p* bands in this case was estimated from RIXS measurements. We note that Ref. 31 presents the energy-resolved XPS *p* and *d* peaks located at 6 and 12 eV, respectively, which gives an energy difference of 6 eV. The difference with our results might stem from calibration techniques: the use of gold foil by Kang *et al.* for calibrating a strong insulator like Mn_{12} is problematic. The differences in the fine structure of the XPS VB most probably stem from different loss of such components of the molecule as CH_3COOH groups or H_2O during pumping.

One can see that the peak of Mn L_3 XES is close to the shoulder of the O $K\alpha(1)$ XES, which can be interpreted as a result of the hybridization between the Mn 3*d* and the O(1) 2*p* states. The C $K\alpha(1)$ and C $K\alpha(2)$ XES are attributed to two different carbon atoms in the carboxylate groups CH_3COO. According to this assignment, the C 2*p* states from different carbon atoms contribute to the features *B* and *C*. The energy difference between C 2*p* and C 2*s* states is about 7 eV. The features *E* and *F* can be attributed to the O 2*s* states.

The valence state of the manganese ions in Mn_{12} can be probed by studying the Mn 3*s* x-ray photoelectron spectra. The spectral splitting of the 3*s* core-level x-ray photoemission spectra in the transition metals and their compounds originates from the exchange coupling between the 3*s* hole and the 3*d* electrons. The magnitude of the splitting is proportional to *S*, where *S* is the local spin of the 3*d* electrons in the ground state. For the 3*d* metal compounds, the calculated 3*s* splitting is more than two times larger than the observed one. It indicates that the observed 3*s* splitting is not likely to be due to the spin exchange only. This fact was explained by the intra-atom correlation effects between the $3s^1 3p^6 3d^n$ and the $3s^2 3p^4 3d^{n+1}$ configurations.[33,34] In addition to the exchange interaction and intra-atom correlation between the 3*d* and 3*s* states, charge-transfer processes must be taken into account. For Cu and Ni oxides, the charge-transfer effect dominates the multiplet effect in 3*s* spectra. With decreasing number of *d* electrons, the role of the charge-transfer processes becomes less important.[35]

The Mn 3*s* spectra of Mn_{12} and several manganese oxides are shown in Fig. 5. According to a simple 3*s*-3*d* Coulomb interaction picture, one can assume that the Mn 3*s* splitting in Mn_{12}, which contains both Mn^{3+} and the Mn^{4+} ions, should be less than in the oxides, which contain only Mn^{3+} ions. In reality the value of the Mn 3*s* splitting for Mn_{12} is about 5.40±0.15 eV, which is nearly equal to the splitting found for oxides with only the Mn^{3+} ions (5.30±0.10 eV; see, e.g., Ref. 36). A similar situation takes place in the colossal magnetoresistance manganites,[36] where doping with Sr^{2+} ions does not change the Mn 3*s* splitting (in a certain concentration region). This effect was explained by the appearance of holes in the O 2*p* states, which leads to the d^4L ground-state configuration, where *L* denotes a hole in the 2*p* orbital of a ligand. One can suggest that in the Mn_{12} compound, the Mn^{4+} ions reflect the atomic configuration d^4L due to the charge transfer from the O 2*p* states to the Mn 3*d* states. This conclusion agrees with the picture observed for the Mn 2*p* x-ray photoelectron spectra of Mn_{12}, where the distance between the main line and the satellite in Mn_{12} (about 23 eV) is similar to that found for manganites. The positions of the XPS Mn 2*p* satellites in Fig. 6 are shown by arrows.

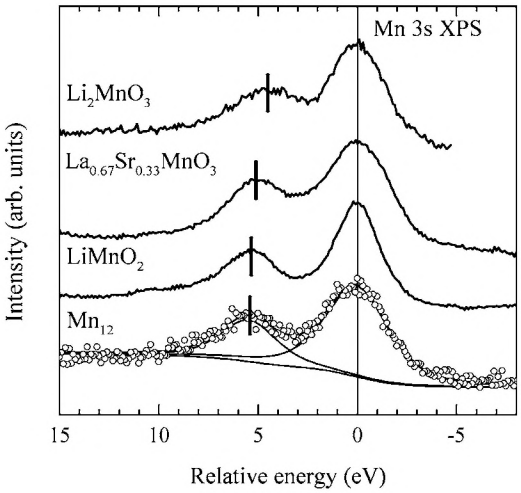

FIG. 5. Mn 3*s* x-ray photoelectron spectra of Mn_{12} and manganese oxides $LiMnO_2$, $La_{0.67}Sr_{0.33}MnO_3$, and Li_2MnO_3. The spectra are given on an energy scale relative to the main maxima of the high-spin components. The deconvolution of the spectrum of Mn_{12} into Gaussian functions is shown by thin solid lines. The positions of the low-spin components for each spectrum are shown by vertical lines.

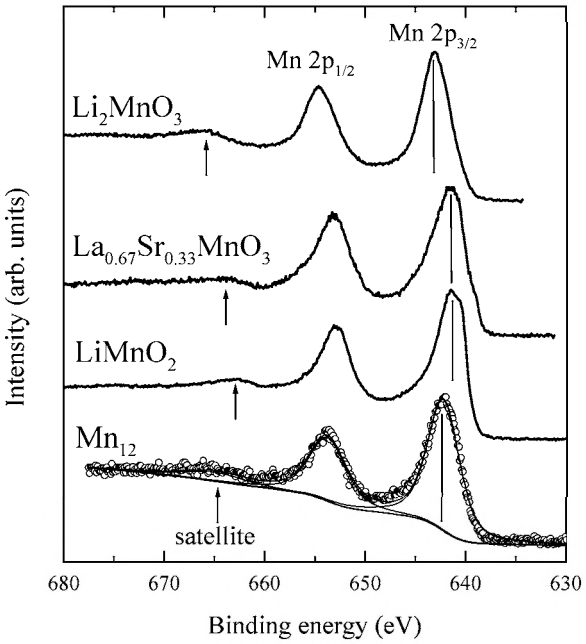

FIG. 6. Mn 2*p* x-ray photoelectron spectra of Mn_{12} and some manganese oxides: $LiMnO_2$, $La_{0.67}Sr_{0.33}MnO_3$, and Li_2MnO_3. The deconvolution of the Mn 2*p* spectrum of Mn_{12} into Gaussian functions is shown by thin solid lines. Positions of the $2p_{3/2}$ main lines and of the satellites are shown by the arrows.

IV. ELECTRONIC STRUCTURE CALCULATIONS AND INTRAMOLECULAR EXCHANGE INTERACTIONS

Our approach to electronic structure calculations of Mn_{12} has been reported previously in Ref. 17. We employ the atomic sphere approximation–linear muffin-tin orbitals LSDA+U method.[11] This method allows taking into account the important electron-electron correlations by considering the on-site Coulomb repulsion between the electrons (quantified by the energy U) and the intra-atomic Hund exchange (quantified by the parameter J). In previous work we performed calculations for the model chemical structure of Mn_{12} where CH_3 groups were replaced by hydrogens. While such an approximation has been used before by several groups,[12–15,17] it appears not always sufficient. Therefore, in the present work we calculate the electronic structure of the full molecule, omitting only the intermolecular water of crystallization and solvate complexes. We take into account 148 atoms in total, which corresponds to about 700 orbitals (including the empty spheres).

For compounds with a small number of atoms per unit cell, the parameters U and J can be accurately determined from first principles (constrained LDA) calculations.[37,38] We performed such calculations for both the reduced structure of Mn_{12} (with CH_3 groups replaced by H), obtaining U =4.2 eV, and for the complete structure, obtaining the value U=3.8 eV. However, for such large systems as Mn_{12} the accuracy of the constrained LDA calculations is much lower: for a given calculation time, the self-consistency conditions for large systems are satisfied with much less precision than for small systems. Therefore, the calculated value of the parameter U should be independently justified by comparison with the experimental data. In the previous work we used optical measurements of the energy gap[39] and found that they are consistent with U=6 eV. However, the estimates for the energy gap differ in different experiments, ranging from 1.7 (Ref. 39) to 0.74 eV (Ref. 40) (the reasons for this difference has been recently analyzed in detail,[41] taking the polyoxovanadate compounds as an example).

In Ref. 22, we briefly reported that the value U=6 eV does not agree with the XES and XPS measurements described above, while U=4 eV results in a good agreement between theory and experiment. Similarly, our constrained LDA calculations gave U close to 4 eV. Another problem has been observed when diagonalizing the spin Hamiltonian of Mn_{12} using the intramolecular exchange parameters determined in Ref. 17 for U=6 eV: these exchange values did not reproduce the ground state with the total spin S=10. This inconsistency has been independently observed, and published in Ref. 42.

In the present paper, we use the XES and XPS measurements presented above for determining the parameter U. These measurements produce a large amount of data, thus making possible a detailed comparison of the theoretically calculated electron density of states with the experimental results. We already employed this approach before to study the V_{15} compound,[18] and the results were encouraging. By performing a similar comparison for Mn_{12}, which is presented below, we found that agreement between theory and experiment is rather good for U=4 eV. Note that this value

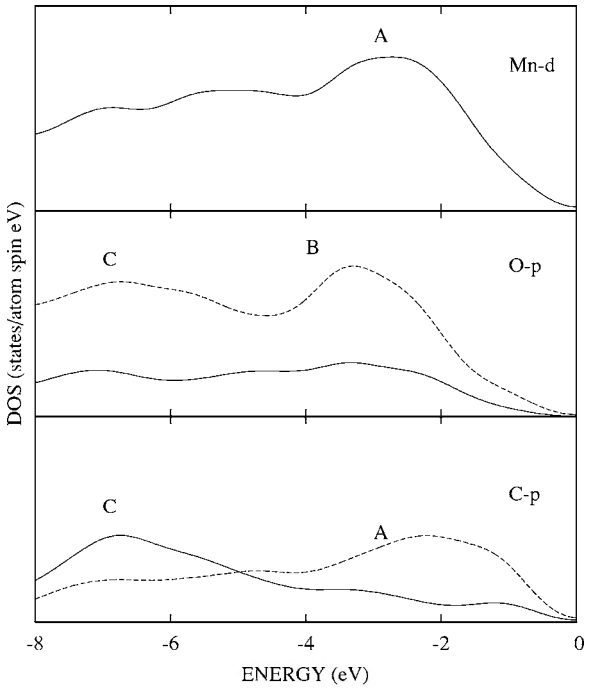

FIG. 7. Calculated projected electronic DOSs for Mn_{12} for Mn 3d (upper panel), different types of O 2p electrons (central panel), and different types of C 2p electrons (lower panel).

is close to the first-principles estimates, 4.2 eV for the reduced structure and 3.8 eV for the complete structure. Moreover, we find that the accuracy of the exchange calculations can be increased by employing the LDA+U scheme instead of the LSDA+U treatment used in our previous work.[17] In the LDA+U case, adopted here, all exchange effects come from the U terms, and the problem of double counting is avoided.

For a detailed comparison with experiments, in Fig. 7 we present the projected electronic density of states for manganese 3d, oxygen 2p, and carbon 2p states, calculated with U=4 eV. The graphs in Fig. 7 were smeared, following the standard practice, by convolution of the calculated energy levels with a Gaussian line of the half-width 0.4 eV, which corresponds to the resolution of the XES and XPS measurements above. The positions of the calculated DOSs given in Fig. 7 agree well with the experimental results presented in Fig. 4. Note that the positions of the "zero" energy are different in Figs. 7, 8, and 4, although the scale is the same. The binding energy (used in Fig. 4) is shifted by about 2 eV with respect to the theoretical energy counted from the Fermi level. This shift takes into account the inaccuracy of the XPS binding energy calibration, which is important for insulating samples due to the charging effect.

It is important to note here that the experimental XPS curves, being mostly determined by the DOS, are strongly affected by the specific matrix elements of the corresponding transitions. Therefore, the positions of the peaks in the XPS spectra should be close to the DOS peaks, but the specific shape of the experimental curves (and, e.g., the heights of the peaks) may considerably differ. At the same time, the calculation of the matrix elements, taking into account the com-

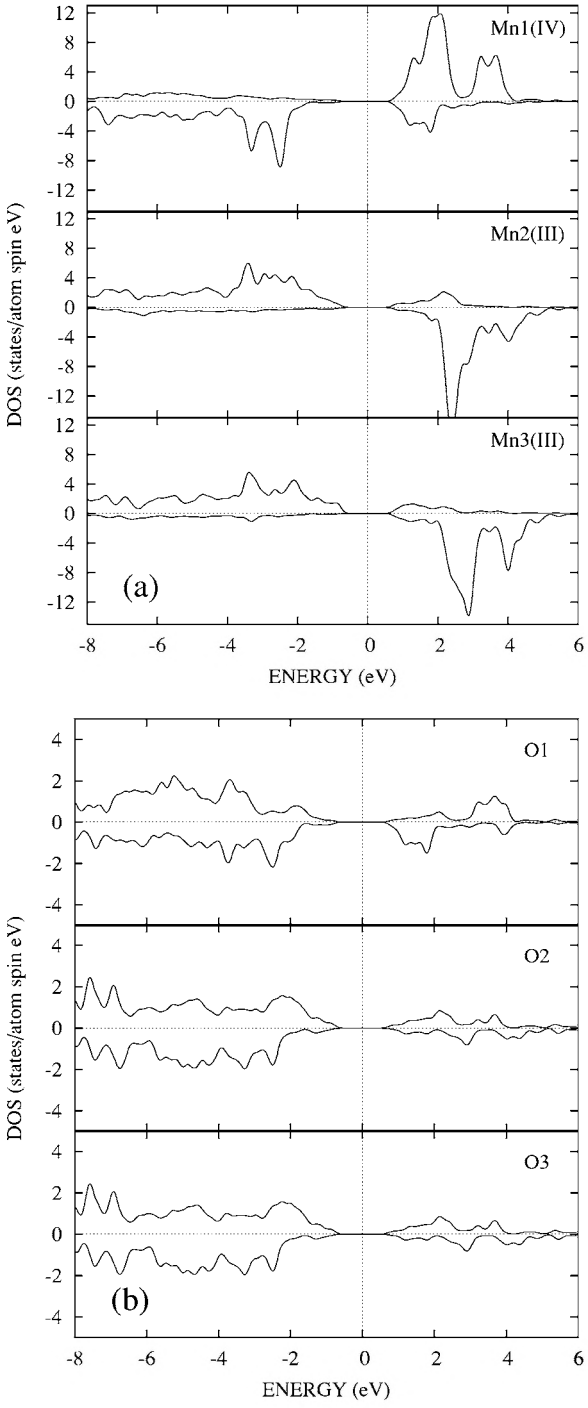

FIG. 8. Calculated projected electronic DOSs for $3d$ states of different manganese atoms (a) and $2p$ states of different oxygen atoms (b) calculated with $U=4$ eV.

plex single-particle and many-particle effects is a very difficult task for such large and complex systems as Mn_{12}, which is far beyond the present capabilities. Therefore, in order to find the parameter U, we focus only on the peak positions and not on their heights.

In the top panel of Fig. 7, the calculated Mn $3d$ DOS is shown. The majority of the Mn $3d$ states are located between (approximately) -1.5 and -4 eV, and the peak (labeled A) corresponds to the experimental peak labeled A on Fig. 4. In

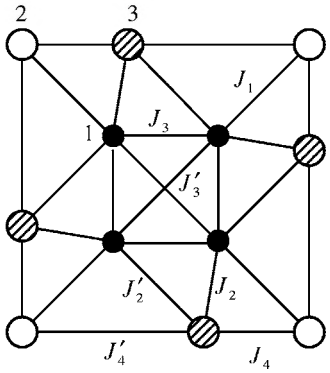

FIG. 9. Sketch of Mn_{12} molecules showing positions of different Mn ions: black circles, Mn1; white circles, Mn2; and dashed circles, Mn3 (denoted by their numbers). The exchange interactions between different ions are shown by solid lines.

the central panel we present the $2p$ DOS for two types of oxygens. The first type (solid line) corresponds to the oxygens from Mn-O-Mn bridges, and the second type (dashed line) includes the oxygens that connect Mn with the ligands (Mn-O-C bridges). The oxygen DOSs exhibit two peaks, denoted as B and C, in correspondence with the experimentally found peaks labeled as B and C in Fig. 4. The peak B in the theoretical DOS is located approximately 1.5 eV lower than peak A in the Mn $3d$ DOS, in agreement with the experimental results. Similarly the peak C in the theoretical O $2p$ DOS is located about 7 eV below the Fermi level, again in good agreement with the experiment. In the bottom panel of Fig. 7, the DOSs of $2p$ states for two types of carbon are shown. The first type of carbons (solid line) are the carbons that are connected to the oxygens, and second type of carbon (dashed line) are the carbons from CH_3 groups. Again, the theoretical carbon $2p$ DOSs are in good agreement with the experimental spectra in Fig. 4. By comparing the XES and XPS spectra with theoretically calculated electron DOSs, we can determine the value of the Coulomb repulsion parameter U with an accuracy of about 0.5 eV.

In Fig. 8 we present in more detail the DOSs for $3d$ states of different manganese atoms and $2p$ states of different oxygen atoms calculated with $U=4$ eV. Each Mn_{12} molecule includes three types of manganese (see Fig. 9): Mn1 are the Mn^{4+} ions located at the corners of the distorted cubane thus forming a distorted tetrahedron, and Mn2 and Mn3 are the Mn^{3+} ions forming an outer "crown" around the central cubane. Mn2 are the nearest neighbors of Mn1, and are located in the same planes as Mn1, while Mn3 are located between two subsequent Mn2, closer to one of them, and farther from the other. There are many different types of oxygen, and Fig. 8 shows the three most interesting types: O1 are the oxygens located inside the central cubane and providing the coupling between different Mn1 ions, O2 are the oxygens which couple the cubane Mn ions (Mn1) with the crown Mn ions (Mn2 and Mn3), and O3 are the oxygens coupling Mn2 with the acetate ligands. In order to show the details of the calculated electronic structure, which are not visible in XES and XPS experiments and in Fig. 7, the graphs were smeared by 0.05 eV. The location of the "zero" energy and the energy scale in this figure are the same as in Fig. 7. The positions of

the calculated DOSs agree well with the experimental results in Fig. 4. The figures show considerable hybridization between the Mn $3d$ states and the corresponding oxygen $2p$ states: the features of the Mn1 DOS are reproduced in the O1 DOS, and the features of the Mn2 and Mn3 DOSs are visible in the O2 and O3 DOSs.

The value $U=4$ eV obtained here is not unusual for manganese, although it is somewhat smaller than, for example, $U=6.9$ eV obtained for MnO. This is explained by the fact that the hybridization between Mn $3d$ and O $2p$ electrons is stronger for Mn_{12} than for MnO. The stronger p-d hybridization leads to less localized wave functions, i.e., to the reduced electron density on a given manganese site, so that the on-site Coulomb repulsion is reduced, resulting in a smaller value of U.[43]

Having calculated the electronic structure of Mn_{12}, we can determine the exchange interactions between different Mn ions inside the molecule, in the same way as in Ref. 17. The intramolecular exchange interactions determine the internal magnetic structure of Mn_{12}, and it is important to investigate whether the exchange parameters can be extracted reliably from the electronic structure calculations. This study is useful for theoretical undestanding of the intramolecular exchanges in Mn_{12}. While considerable research effort has been focused in this area[17,42,44–47] and a lot of valuable information has been obtained, a clear theoretical picture is still lacking.

We assume the following form of the exchange spin Hamiltonian:

$$H = \sum_{i,j} J_{ij} \mathbf{S}_i \cdot \mathbf{S}_j, \tag{1}$$

where the summation goes over all spins, and $J_{ij}=J_{ji}$. This definition implies that the exchange energy for a pair of spins $\mathbf{S}_1$ and $\mathbf{S}_2$ is $2J_{12}\mathbf{S}_1 \cdot \mathbf{S}_2$. Since most Mn centers are very far from each other, most exchanges are very weak, 1–2 K, which is within the range of accuracy of our calculations, and therefore should be neglected. Only a handful of exchange parameters have non-negligible values, and many of them are equal to each other due to the high symmetry of the Mn_{12} molecule. Therefore, all the exchange couplings can be divided into several groups, as shown in Fig. 9. The parameter J_1 describes the exchange between Mn1 and the nearest Mn2 ion, coupled through two oxygen bridges. J_2 and J_2' correspond to the exchange of Mn1 and Mn3 ions coupled by a single oxygen bridge. Every Mn3 ion is coupled to two Mn1 ions: one Mn1 is located closer to a given Mn3, with corresponding coupling parameter J_2, and the other Mn1 is located farther away, with corresponding coupling J_2'. The parameters J_3 and J_3' describe the exchange between different Mn1 ions (see also Ref. 17): J_3 corresponds to Mn1 ions located closer to each other, while J_3' corresponds to Mn1 located farther from each other. Finally, J_4 corresponds to Mn2 and Mn3 located closer to each other, and J_4' corresponds to Mn2 and Mn3 located farther from each other.

As shown our previous work,[17] the exchange parameters change appreciably (by about 30%) with changes in the magnetic structure of the molecule, which means that the model of isotropic Heisenberg exchange is only semiquantitatively valid in Mn_{12}. Correspondingly, other sources of errors, such as the finite number of k points used for integration over the Brillouin zone, are not as important. In most calculations the number of k points is 4 per the irreducible part of the Brillouin zone, and the test calculations with larger number of k points show that by changing the number of k points from 4 to 134 (per irreducible part of the Brillouin zone), the exchange parameters vary only by ~7%. Similarly, a moderate variation of U leads to moderate variation of the exchanges; the exchange parameters calculated for $U=3.5$, 4.0, and 4.5 eV, are presented in Table I.

TABLE I. Dependence of the calculated exchange parameters (in kelvin) and the electronic structure gap (in eV) on small variation of the Columb repulsion parameter U (in eV).

U	3.5	4.0	4.5
J_1	52	50	48
J_2	44	43	40
J_2'	42	37	32
J_3	12	8	6
J_3'	4	3	3
J_4	11	10	9
J_4'	8	6	5
Ground state spin S	10	10	10
Gap (eV)	1.31	1.40	1.46

In order to check whether the calculated exchanges are reasonable, we have performed an exact diagonalization of the exchange spin Hamiltonian of Mn_{12}. The dimension of the Hilbert space is 10^8, but the Hamiltonian (1) commutes with the operator of the z projection of the molecule's total spin, S_z, and it is sufficient to diagonalize only the subspace with $S_z=0$ in order to get the complete eigensystem. In this paper we are interested only in the ground state, so that the diagonalization has been performed using the Davidson algorithm[48] which efficiently determines several lowest eigenvectors and eigenvalues. The diagonalization demonstrated that the exchange parameters calculated with all three values of $U=3.5$, 4.0, and 4.5 eV, lead to the $S=10$ ground state.

In spite of this agreement, a word of caution is in place. The $S=10$ ground state of the Mn_{12} is a result of competition between different antiferromagnetic exchanges, and the properties of the ground state, as well as of the few first excited states, are very sensitive to the exact values of the exchange parameters.[42,47] Although the exchange interactions calculated here are reasonably close to those reported earlier,[42] modification of the exchanges from Table I by a few kelvin, or taking into account the weaker exchange interactions between more distant Mn ions (which have values of 1–2 K, and thus cannot be reliably determined from the electronic structure calculations), can noticeably change the lowest-energy states. This problem for Mn_{12} is in sharp contrast with the analogous problem for V_{15} magnetic molecules,[19,20] where the Heisenberg approximation for exchange interactions works very well, and the exchanges obtained from the electronic structure calculation for V_{15} can

be directly plugged into the relevant spin Hamiltonian to produce a very good agreement with experimental results. Due to the restricted validity of the Heisenberg approximation and non-negligible (a few kelvin) precision of the exchange parameters, the results of the electronic structure calculations for Mn_{12} should be cautiously considered as the estimates of the "actual" exchange parameters. Moreover, the anisotropic interactions (Dzyaloshinski-Moriya coupling, single-ion anisotropy) are strong in Mn_{12}, and affect significantly the properties of the low-lying states. Therefore, theoretical understanding of the spin Hamiltonian of Mn_{12} and comparison with available experimental data requires a separate detailed investigation, which will be presented elsewhere.[47]

V. CONCLUSIONS

We used site-selective and element-specific resonant inelastic x-ray scattering and x-ray photoelectron spectroscopy to study the electronic structure and electron interaction effects in the molecular magnet Mn_{12}. The experimental data have been compared with electronic structure calculations (using the LSDA+U technique) taking into account the on-site Coulomb interaction. The separation between the p and d bands of 1.8 eV, which has been found in the experiment, is in agreement with theoretical results. Good agreement with the experimental spectra is obtained for $U=4$ eV which also gives reasonable values for band gap and magnetic moments of the manganese ions. We also calculated the intramolecular exchange interactions and used them as an input for diagonalization of the isotropic Heisenberg Hamiltonian. The calculated exchanges correctly reproduce the ground state with the total spin $S=10$. Therefore, we conclude that the value of $U=4$ eV is a reasonable estimate for the Coulomb on-site repulsion parameter. However, for a detailed understanding of the spin Hamiltonian spectrum of Mn_{12}, a more detailed study is needed.

ACKNOWLEDGMENTS

Funding by the Research Council of the President of the Russian Federation (Grants No. NSH-4192.2006.2 and No. NSH-4640.2006.2), Russian Foundation for Basic Research (Projects No. 05-02-16438 and No. 05-02-17704), NATO Collaborative Linkage Grant No. PST.CLG.978044, the Natural Sciences and Engineering Research Council of Canada (NSERC), and the Canada Research Chair Program is gratefully acknowledged. The work is partially supported by the Netherlands Organization for Scientific Research (Grant No. NWO 047-008-16). This work was partially carried out at Ames Laboratory, which is operated for the U.S. Department of Energy by Iowa State University under Contract No. W-7405-82 and was supported by the Director of the Office of Science, Office of Basic Research of the U.S. Department of Energy. The work at the Advanced Light Source at Lawrence Berkeley National Laboratory was supported by U.S. Department of Energy (Contract No. DE-AC03-76SF00098). N.D. acknowledges NSF, Grant No. NIRT-DMR 0506946.

[1] T. Lis, Acta Crystallogr., Sect. B: Struct. Crystallogr. Cryst. Chem. **36**, 2042 (1980).
[2] J. R. Friedman, M. P. Sarachik, J. Tejada, and R. Ziolo, Phys. Rev. Lett. **76**, 3830 (1996).
[3] L. Thomas, F. Lionti, R. Ballou, D. Gatteshi, R. Sessoli, and B. Barbara, Nature (London) **383**, 145 (1996).
[4] *Quantum Tunneling of Magnetization—QTM'94*, edited by L. Gunther and B. Barbara, NATO Advanced Studies Institute, Series E: Applied Science (Kluwer, Dordrecht, 1995), Vol. 301.
[5] E. M. Chudnovsky and L. Gunther, Phys. Rev. Lett. **60**, 661 (1988).
[6] V. V. Dobrovitski and A. K. Zvezdin, Europhys. Lett. **38**, 377 (1997); L. Gunther, *ibid.* **39**, 1 (1997).
[7] W. Wernsdorfer, R. Sessoli, A. Caneschi, D. Gatteschi, and A. Cornia, Europhys. Lett. **50**, 552 (2000).
[8] K. Terakura, A. R. Williams, T. Oguchi, and J. Kubler, Phys. Rev. Lett. **52**, 1830 (1984).
[9] A. Svane and O. Gunnarsson, Phys. Rev. Lett. **65**, 1148 (1990).
[10] A. I. Lichtenstein and M. I. Katsnelson, Phys. Rev. B **57**, 6884 (1998).
[11] V. I. Anisimov, F. Aryasetiawan, and A. I. Lichtenstein, J. Phys.: Condens. Matter **9**, 767 (1997).
[12] Z. Zeng, D. Guenzburger, and D. E. Ellis, Phys. Rev. B **59**, 6927 (1999).
[13] M. R. Pederson and S. N. Khanna, Phys. Rev. B **60**, 9566 (1999).
[14] Kyungwha Park and Mark R. Pederson, Phys. Rev. B **70**, 054414 (2004).
[15] Kyungwha Park, Mark R. Pederson, and C. Stephen Hellberg, Phys. Rev. B **69**, 014416 (2004).
[16] J. Kortus, C. S. Hellberg, and M. R. Pederson, Phys. Rev. Lett. **86**, 3400 (2001).
[17] D. W. Boukhvalov, A. I. Lichtenstein, V. V. Dobrovitski, M. I. Katsnelson, B. N. Harmon, V. V. Mazurenko, and V. I. Anisimov, Phys. Rev. B **65**, 184435 (2002).
[18] D. W. Boukhvalov, E. Z. Kurmaev, A. Moewes, D. A. Zatsepin, V. M. Cherkashenko, S. N. Nemnonov, L. D. Finkelstein, Yu. M. Yarmoshenko, M. Neumann, V. V. Dobrovitski, M. I. Katsnelson, A. I. Lichtenstein, B. N. Harmon, and P. Kögerler, Phys. Rev. B **67**, 134408 (2003).
[19] D. W. Boukhvalov, V. V. Dobrovitski, M. I. Katsnelson, A. I. Lichtenstein, B. N. Harmon, and P. Kögerler, Phys. Rev. B **70**, 054417 (2004).
[20] D. W. Boukhvalov, V. V. Dobrovitski, M. I. Katsnelson, A. I. Lichtenstein, B. N. Harmon, and P. Kögerler, J. Appl. Phys. **93**, 7080 (2003).
[21] A. I. Lichtenstein, V. I. Anisimov, and M. I. Katsnelson, in *Electronic Structure and Magnetism of Complex Materials*, edited by D. J. Singh and D. A. Papaconstantopoulos (Springer, Berlin 2003), p. 101.
[22] D. W. Boukhvalov, E. Z. Kurmaev, A. Moewes, M. V.

Yablonskikh, S. Chiuzbăian, V. R. Galakhov, L. D. Finkelstein, A. Neumann, M. I. Katsnelson, V. V. Dobrovitski, and A. L. Lichtenstein, in Proceedings of the Ninth International Conference on Electronic Spectroscopy and Structure, Uppsala, Sweden, 2003; J. Electron Spectrosc. Relat. Phenom. **137**, 735 (2004).

[23] J. A. A. J. Perenboom, J. S. Brooks, S. Hill, T. Hathaway, and N. S. Dalal, Phys. Rev. B **58**, 330 (1998).

[24] A. Kotani and S. Shin, Rev. Mod. Phys. **73**, 203 (2001).

[25] E. Z. Kurmaev, S. Stadler, D. L. Ederer, Y. Harada, S. Shin, M. M. Grush, T. A. Callcott, R. C. C. Perera, D. A. Zatsepin, N. Ovechkina, M. Kasai, Y. Tokura, T. Takahashi, K. Chandrasekaran, R. Vijayaraghavan, and U. V. Varadaraju, Phys. Rev. B **57**, 1558 (1998).

[26] S. M. Butorin, J. Guo, N. Wassdahl, E. J. Nordgren, J. Electron Spectrosc. Relat. Phenom. **235**, 110 (2000).

[27] H. W. Skinner, T. G. Bullen, and J. Jonston, Philos. Mag. **45**, 1070 (1954).

[28] V. R. Galakhov, E. Z. Kurmaev, and V. M. Cherkashenko, Izv. Akad. Nauk SSSR, Ser. Fiz. **49**, 1513 (1987).

[29] V. I. Grebennikov, Phys. Met. Metallogr. **89**, 425 (2000).

[30] V. I. Grebennikov, V. R. Galakhov, L. D. Finkelstein, N. A. Ovechkina, and E. Z. Kurmaev, Phys. Solid State **45**, 1048 (2003).

[31] J.-S. Kang, J. H. Kim, Y. J. Kim, W. S. Jeon, D.-Y. Jung, S. W. Han, K. H. Kim, K. J. Kim, and B. S. Kim, J. Korean Phys. Soc. **40**, L402 (2002); J. H. Kim, S. C. Wi, J.-S. Kang, Duk-Young Jung, S. W. Han, and K. H. Kim, J. Magn. Magn. Mater. **272-276**, e735 (2004).

[32] J.-H. Guo, Y. Luo, A. Augustsson, J.-E. Rubensson, C. Såthe, H. Ågren, H. Siegbahn, and J. Nordgren, Phys. Rev. Lett. **89**, 137402 (2002).

[33] P. S. Bagus, A. J. Freeman, and F. Sasaki, Phys. Rev. Lett. **30**, 850 (1973).

[34] E.-K. Viinikka and Y. Öhrn, Phys. Rev. B **11**, 4168 (1975).

[35] K. Okada and A. Kotani, ISSP Technical Report, Series A, No. 2541, 1992 (unpublished); K. Okada and A. Kotani, J. Phys. Soc. Jpn. **61**, 4619 (1992); K. Okada, A. Kotani, and B. Thole, J. Electron Spectrosc. Relat. Phenom. **58**, 325 (1992).

[36] V. R. Galakhov, M. Demeter, S. Bartkowski, M. Neumann, N. A. Ovechkina, E. Z. Kurmaev, N. I. Lobachevskaya, Ya. M. Mukowskii, J. Mitchell, and D. L. Ederer, Phys. Rev. B **65**, 113102 (2002).

[37] O. Gunnarsson, O. K. Andersen, O. Jepsen, and J. Zaanen, Phys. Rev. B **39**, 1708 (1989).

[38] V. I. Anisimov and O. Gunnarsson, Phys. Rev. B **43**, 7570 (1991).

[39] S. M. Oppenheimer, A. B. Sushkov, J. L. Musfeldt, R. M. Achey, and N. S. Dalal, Phys. Rev. B **65**, 054419 (2002).

[40] J. M. North, D. Zipse, N. S. Dalal, E. S. Choi, E. Jobiliong, J. S. Brooks, and D. L. Eaton, Phys. Rev. B **67**, 174407 (2003).

[41] A. Barbour, R. D. Luttrell, J. Choi, J. L. Musfeldt, D. Zipse, N. S. Dalal, D. W. Boukhvalov, V. V. Dobrovitski, M. I. Katsnelson, A. I. Lichtenstein, B. N. Harmon, and P. Kögerler, Phys. Rev. B **74**, 014411 (2006).

[42] G. Chaboussant, A. Sieber, S. Ochsenbein, H.-U. Güdel, M. Murrie, A. Honecker, N. Fukushima, and B. Normand, Phys. Rev. B **70**, 104422 (2004).

[43] V. I. Anisimov, J. Zaanen, and O. K. Andersen, Phys. Rev. B **44**, 943 (1991).

[44] R. Sessoli, H.-L. Tsai, A. R. Shake, S. Wang, J. B. Vincent, K. Folting, D. Gatteschi, G. Christou, and D. N. Hendrickson, J. Am. Chem. Soc. **115**, 1804 (1993).

[45] M. I. Katsnelson, V. V. Dobrovitski, and B. N. Harmon, Phys. Rev. B **59**, 6919 (1999).

[46] V. V. Platonov, B. Barbara, A. Caneschi, D. A. Clark, C. M. Fowler, D. Gatteschi, J. D. Goettee, I. A. Lubashevsky, A. A. Mukhin, V. I. Plis, A. I. Popov, D. G. Rickel, R. Sessoli, O. M. Tatsenko, and A. K. Zvezdin (unpublished); B. Barbara, D. Gatteschi, A. A. Mukhin, V. V. Platonov, A. I. Popov, A. M. Tatsenko, A. K. Zvezdin, in *Proceedings of the Seventh International Conference on Megagauss Magnetic Field Generation and Related Topics, Sarov, 1996* (1997), p. 853.

[47] M. Al-Saqer, V. V. Dobrovitski, D. W. Boukhvalov, M. I. Katsnelson, A. I. Lichtenstein, and B. N. Harmon (unpublished).

[48] E. R. Davidson, J. Comput. Phys. **17**, 87 (1975); E. R. Davidson, Comput. Phys. Commun. **53**, 49 (1989).